

AD-A094 343

INDIANA UNIV AT BLOOMINGTON DEPT OF CHEMISTRY F/6 20/9
OPERATIONAL CHARACTERISTICS OF A HELIUM MICROWAVE-INDUCED PLASM--ETC(U)
JAN 81 A T ZANDER, G M HIEFTJE N00014-76-C-0838
TR-30 NL

UNCLASSIFIED

1 of 1
49,424,247



END
DATE
FILMED
2 -81
DTIC

UNCLASSIFIED

SECURITY CLASSIFICATION OF THIS PAGE (When Data Entered)

12
B 5

REPORT DOCUMENTATION PAGE

READ INSTRUCTIONS
BEFORE COMPLETING FORM

| | | | |
|---|--|--|-------------------------------|
| 1. REPORT NUMBER THIRTY 1071-37, 38 | | 2. GOVT ACCESSION NO. 4D-AC94343 | 3. RECIPIENT'S CATALOG NUMBER |
| 4. TITLE (and Subtitle) Operational Characteristics of a Helium Microwave-Induced Plasma at Atmospheric Pressure, | | 5. TYPE OF REPORT & PERIOD COVERED Interim Technical Report, | |
| 7. AUTHOR(s) Andrew T. Zander and Gary M. Hieftje | | 8. CONTRACT OR GRANT NUMBER(s) N-14-C-0838 | |
| 9. PERFORMING ORGANIZATION NAME AND ADDRESS Department of Chemistry Indiana University Bloomington, Indiana 47405 | | 10. PROGRAM ELEMENT, PROJECT, TASK AREA & WORK UNIT NUMBERS NR 51-622 | |
| 11. CONTROLLING OFFICE NAME AND ADDRESS Office of Naval Research Washington, D.C. | | 12. REPORT DATE January 26, 1981 | |
| 14. MONITORING AGENCY NAME & ADDRESS (if different from Controlling Office) 15. SECURITY CLASS. (of this report) UNCLASSIFIED | | 13. NUMBER OF PAGES 15 | |
| 16. DISTRIBUTION STATEMENT (of this Report) Approved for public release; distribution unlimited | | 15a. DECLASSIFICATION/DOWNGRADING SCHEDULE | |
| 17. DISTRIBUTION STATEMENT (of the abstract entered in Block 20, if different from Report) THIS DOCUMENT IS BEST QUALITY AVAILABLE. THE COPY FURNISHED TO DDC CONTAINED A SIGNIFICANT NUMBER OF PAGES WHICH DO NOT REPRODUCE LEGIBLY. | | | |
| 18. SUPPLEMENTARY NOTES Prepared for publication in ICP Newsletter | | | |
| 19. KEY WORDS (Continue on reverse side if necessary and identify by block number) microwave plasma emission spectroscopy multielement analysis excitation source | | | |
| 20. ABSTRACT (Continue on reverse side if necessary and identify by block number) The microwave-induced helium plasma generated at atmospheric pressure in the TM ₀₁₀ resonant cavity is attractive as an excitation source for emission spectrometry. The efficiency of the cavity produces an extremely high energy-density plasma and its short longitudinal dimension permits close spatial and photometric monitoring system proximity between the plasma and different types of sampling devices. Examination of the electron density, excitation temperature and rotational temperature in this microwave plasma reveals its unusual character and suggests certain mechanisms of operation. | | | |

AD A094343

DDC FILE COPY

DD FORM 1473 1 JAN 73

EDITION OF 1 NOV 65 IS OBSOLETE
S/N 0102-014-6

UNCLASSIFIED

176665

81 2

2

010

OFFICE OF NAVAL RESEARCH

Contract N14-76-C-0838

Task No. NR 051-622

TECHNICAL REPORT NO. 30

OPERATIONAL CHARACTERISTICS OF A HELIUM MICROWAVE-
INDUCED PLASMA AT ATMOSPHERIC PRESSURE

by

Andrew T. Zander and Gary M. Hieftje

Prepared for Publication

in

ICP NEWSLETTER

Indiana University

Department of Chemistry

Bloomington, Indiana 47405

January 26, 1981

Reproduction in whole or in part is permitted for
any purpose of the United States Government

Approved for Public Release; Distribution Unlimited

DISCLAIMER NOTICE

**THIS DOCUMENT IS BEST QUALITY
PRACTICABLE. THE COPY FURNISHED
TO DTIC CONTAINED A SIGNIFICANT
NUMBER OF PAGES WHICH DO NOT
REPRODUCE LEGIBLY.**

INTRODUCTION

Microwave-induced plasmas (MIP) have been of continuing interest as atomic emission excitation sources for spectrochemical analysis(1,2). In accord with increased interest in induction plasmas in general, undoubtedly spurred by advancements with RF ICP's, the MIP has recently received more attention than it has had in the past. However, the resurgence of interest has been more directly the result of two independent factors. As the popularity of microwave ovens has increased, the availability of high quality, high power magnetrons to supply cw microwave power at 2450 MHz has become wider. Thus, laboratory and research versions of microwave power supplies are inexpensive and more readily obtainable. The second factor was the introduction of the TM_{010} resonant cavity to analytical spectroscopists by Beenakker in 1976(3). In that and following publications(2-8) the TM_{010} cavity was described in detail and shown to possess some very useful operational characteristics and to have the capability to excite most nonmetals and all of the halogens(9-14).

The features of the TM_{010} cavity which make it advantageous for use in atomic emission experiments are numerous. The dimensions of the cavity are such that the discharge is constrained to a very small volume. It is within this volume that all of the input power is concentrated. The result is that the energy density in the location of the discharge is greatly increased relative to other cavity types. This allows the self-ignition and straight⁵/forward operation of an atmospheric pressure discharge in helium. The advantages accruing from the use of helium as the support gas are lower overall background spectrum, higher metastable species energy, and a more diffuse plasma which is less prone to erratic movements and dislocations during sample injection. The configuration of the TM_{010} cavity is such that the MIP is within a few millimeters of either end of the cavity, which permits simpler and more direct access to the discharge. This arrangement eliminates a multitude of sample transport problems and improves the efficiency of radiation collection from the plasma. The MIP is more easily viewed in the axial

direction, eliminating signal degradation which is encountered as the chamber wall, through which radial observation must be made, erodes with use. The TM_{010} cavity seems to allow more efficient transfer of power to the discharge as evidenced by the lack of required cavity cooling apparatus. Finally, the MIP operates with support gas flow rates which are economical of He usage.

In the present studies excitation and kinetic temperatures and the electron density were spatially profiled to define some of the principal operating characteristics of the helium MIP at atmospheric pressure. Previously reported portions of this work have indicated possible flow rate/power level trade-offs for optimal signal generation, various signal gradients in the MIP, and suggested reduction of the MIP excitation capability by material injected into the plasma from wall erosion(15-17). More extensive reports have appeared which addressed the character of various low and high pressure microwave discharges(18-24). In a number of cases attempts to elucidate excitation mechanisms and pathways in MIP's were presented. The material presented here is meant to further characterize the atmospheric pressure helium MIP without, at this time, proposing such mechanistic schemes.

EXPERIMENTAL

The TM_{010} microwave resonant cavity, its tuning characteristics, and our inert gas manifold system have been described in detail elsewhere(8,15-17). The optical system imaged the axially-viewed plasma, without magnification, on the entrance slit of an echelle monochromator(SpectraMetrics, Inc., Andover, MA) which had been modified for wavelength modulation and was motorized for scanning. Entrance and exit apertures were 50 μ wide and 200 μ high. The monochromator was used in the single channel mode with an EMI 6256B photomultiplier tube(EMI Gencom, Plainview, NY) with an S-13 response. The photoanodic current was input to a microvolt ammeter(Model 150, Keithley, Co., Cleveland, OH) and recorded on a strip chart recorder(Heath, Co.,

4

Benton Harbor, MI). Conditions employed here were similar or very close to those routinely used for MIP-AES. The chamber used to contain the MIP was an approximately 3cm long section of quartz tubing of 3mm i.d. and 5mm o.d. The tubing did not extend outside the body of the cavity.

Applied power levels which are reported were taken as the difference between readings of the forward and reflected power, both indicated on the generator power meter. Clearly, this value is not necessarily the actual power dissipated in the discharge; some is lost through radiation and impedance mismatching between the transmission line and the changing reactance of the plasma. However, the determination of the power expended in the discharge would require substantially more complex experimentation. An examination of recent literature showed that no reports thus far have attempted to define the power transferred solely to the MIP.

Data were taken at power levels from 60W to 350W. Previous reports have examined the effect of applied power level on MIP temperatures and densities(15-17); ^dData reported here are for 100W plasmas only. The parametric profiles and trends at this power level are typical of data at other power levels up to about 250W. It should be noted that since the TM_{010} cavity affords such high energy density in the MIP that the 100W level reported here is equivalent to much higher levels in other types of cavities. Moreover, preliminary studies indicate that applied power above 300W does not lead to increased analyte emission intensity, makes the MIP more difficult to control, and severely shortens the lifetime of replaceable components(15). i/d

The cavity was mounted on a two-dimensional positioning stand which allowed focussing of any point on the MIP face on the monochromator entrance aperture. The spatial resolution was approximately $200 \mu^m$. Relative emission line intensities and line profile scans were obtained across the face of the axially-viewed plasma. Only at lower power levels (below about 70W) is the MIP cylindrically symmetrical with the plasma chamber. In all other cases the plasma does not reside in the center of the 2
m/

chamber along the axial dimension, and is radially asymmetric in intensity. Although the plasma is relatively short compared to other types of MIP's it is not so short as to assume homogeneity in temperature and electron density along the longitudinal coordinate. Since this study did not address the more difficult task of accurately measuring intensities ~~in the radial direction, so as to obtain~~ longitudinal profiles, it must be kept in mind that the axially measured intensities are averaged readings along the line of sight. The excitation temperatures were obtained from two thermometric species: Fe analyte atoms and He support gas atoms. Measurements of the relative intensities of well-documented lines of these species afforded temperature determinations by the slope method. The thermometric species used for rotational temperature determinations was the C₂ molecule, obtained from injection of a continuous flow of acetone vapor. The electron density was calculated from the width of the Stark-broadened 486.1nm H_g line. Hydrogen is present in the MIP from organic impurity components of the high purity He used, from entrained atmospheric water vapor, and from material eroded from the chamber walls.

For temperature measurements it is clear that the values obtained can only be as reliable as the values of the atomic transition probabilities which are used in the determinations. These values are reliably known only to about 20-25%. It should be kept in mind that when working in plasmas suspected to be far from thermodynamic equilibrium, as this MIP is, relative line intensity temperature determinations are at best approximate. Consequently, the absolute values of the temperatures reported are of less significance than the profiles and trends of these variables.

RESULTS AND DISCUSSION

It was observed in all experiments that as the flow rate increased the center of the plasma moved closer to the chamber wall. The chamber, which is continually eroding at all power

levels and flow rates, ^{apparently} undergo ~~of~~ increased erosion at higher He input rates, ejecting more material into the MIP. This effect is suspected to occur because of relatively ^{by} greater power absorption by the chamber wall at increased flow rates. Power absorption by the wall generally increases as the cavity becomes detuned, so that a tuning dependence on input flow rate might be inferred. It is suggested that this would be due to an adverse change in the reactive load nature of the MIP as the flow rate rises, for example, through increased flow turbulence. In any case, the material ejected into the plasma is transported out of the chamber through the MIP. The establishment of a route for the flow of material may then be the cause of MIP stabilization on the wall. Alternatively, the erosion of the chamber wall may lead not to just material injection into the MIP; but to increased production of charge-carrying species, the entrance of which into the MIP causes it to stabilize at the region of their production. The observation of the attachment of the MIP ends to the wall, as evidenced by distortion of the normally symmetrical plasma, requires that species which are extractable from the chamber wall, for example, Si, OH, H, O, Al, B, N (depending upon the chamber material used) always be considered in the characterization of the MIP.

In Figure 1 are plotted the He excitation temperature profiles, $T_e(\text{He})$, at different flow rates of support gas for a 100W He MIP. The $T_e(\text{He})$ profiles at all flow rates exhibit the same overall shape. It is clear that the lowest temperatures are at the MIP center. (The MIP center is defined as the visibly brightest spot of the plasma; its location is noted on each figure.) There is a region external to the core of the MIP at which $T_e(\text{He})$ is highest. The values of $T_e(\text{He})$ at the MIP center compare well with previously reported values. The lower $T_e(\text{He})$ at the plasma center might be the result of energy loss to the erosion species in the plasma, or de-excitation of the He by these same species. Further studies to characterize the species present are necessary to support this

view. The high values of $T_e(\text{He})$ external to the MIP core tend to indicate that analyte excitation might be optimum outside the MIP. $T_e(\text{He})$ at all points drops as the flow rate increases. This trend may be due to a decrease in species residence time in the excitation volume as the flow rate increases. All this occurs at the same time the plasma becomes more elongated at higher flows. The elongation of the plasma tends to support the view that excitation species are being swept out of the chamber. The total plasma volume remains approximately unchanged.



In Figure 2 are plotted the excitation temperatures at different flow rates, determined using Fe as the thermometric species, $T_e(\text{Fe})$. The profiles are nearly flat across the visible plasma core. $T_e(\text{Fe})$ is lowest external to the core, different in character to $T_e(\text{He})$. As the flow rate rises the profiles rise at all points, also opposite the behavior of $T_e(\text{He})$. The temperature closest to the wall rises most rapidly. There may be some correlation of this rise with the increase wall erosion observed, but it is unclear at this time what it might be. These profiles would tend to indicate that analyte excitation might be optimum at the plasma center.



Electron density profiles across the plasma face were observed to be essentially flat. The values of the electron density obtained were between $1.0 \times 10^{14} \text{ cm}^{-3}$ and $1.6 \times 10^{14} \text{ cm}^{-3}$.

A qualitative assessment of the ionization temperature through the use of the Saha equation indicated T_i values were also essentially unchanged across the MIP. The values estimated were reasonably close to other reported values(25). Further study is warranted for a quantitative assessment of the ionization temperature.

In Figure 3 are plotted the relative line intensity profiles for the Fe 371.994nm ground state line and the 287.234nm nonresonance line (levels 42532.76 cm^{-1} to 7728.071 cm^{-1}). The Fe was injected continuously into the MIP with a microarc sampling device(8,26). It is observed that the profiles of the two lines are distinctly different in shape. At each flow

rate the maximum of the resonance line intensity is external to the MIP center and corresponds roughly with the peak excitation temperature for He (cf. Figure 2). In contrast, the maximum of the nonresonance line intensity is approximately at the MIP center. The minima for each profile are similarly opposite in character. This behavior suggests that higher energy levels of an analyte atom are highly populated in the plasma core. The higher intensities of the resonance line found external to the plasma core follow the $T_e(\text{He})$, and this fact seems to suggest different excitation mechanisms inside, and outside the plasma core. If it is assumed, for example, that He metastables are principally responsible for analyte excitation (from the ground state, at least), then the low resonance line intensity within the MIP might be due to a metastable quenching by wall-erosion material; or there might be some suprathreshold mechanism in effect. This behavior is still in the preliminary stages of examination.

All of the ^{He excitation} profiles decrease in magnitude at all points as the flow rate increases. The amount of decrease at any specific point is not directly correlated with the amount of flow rate increase. However, a possible explanation for this overall trend is a reduction of the residence time for all types of species involved in excitation as the flow rate increases.

The relative values of the line intensities at various positions in the chamber and under varying conditions have not been completely examined at this time. More extensive study in this direction is planned and is expected to provide further insight into the workings of this MIP.

The marked differences in the values of the various temperature types at all points and among the profiles suggests strongly that the atmospheric pressure microwave discharge is nonthermal. The existence of a peaked $T_e(\text{He})$ profile with a minimum at the MIP center in contrast to the relatively featureless $T_e(\text{Fe})$ profile is suspected to be due, at least in part, to a greater effect of the chamber wall erosion species on $T_e(\text{He})$.

*Should consider
excitation from
 $T_e(\text{He}) + \text{Fe}$
excitation profiles
(in app. direction
+ dist. shape)
 $T_e(\text{Fe})$ etc.
7/10/54
JCS*

This proposition is suggestive of different mechanistic paths for each species in the plasma. However, further elucidation of any plasma excitation mechanism will require species population studies and emission line ratio studies. Some progress toward clarifying such a mechanism has been reported(22,23).

CONCLUSIONS

The atmospheric pressure He MIP generated in the TM_{010} cavity has been shown to possess rather complex temperature and emission intensity character in a chamber about three times larger than the plasma volume. Wall effects on the MIP probably quench the plasma core; however, other more complex mechanisms may be in effect.

ACKNOWLEDGEMENT

Supported in part by the Office of Naval Research and by the National Science Foundation through grants CHE 77-22152 and CHE 79-18073.

LITERATURE CITED

1. Greenfield, S., McGeachie, H. McD., Smith, P. B., *Talanta*, 1972, 22, 553.
2. Skogerboe, R. K., Coleman, G. N., *Anal. Chem.*, 1976, 48, 611A.
3. Beenakker, C. I. M., *Spectrochim. Acta*, 1976, 31B, 483.
4. Beenakker, C. I. M., *Spectrochim. Acta*, 1977, 32B, 173.
5. Beenakker, C. I. M., Boumans, P. W. J. M., *Spectrochim. Acta*, 1978, 33B, 53.
6. Beenakker, C. I. M., Bosman, B., Boumans, P. W. J. M., *Spectrochim. Acta*, 1978, 33B, 373.
7. Van Dalen, J. P. J., DeLezenne Coulander, P. A., DeGalan, L., *Spectrochim. Acta*, 1978, 33B, 545.
8. Zander, A. T., Hieftje, G. M., *Anal. Chem.*, 1978, 50, 1257.
9. Quimby, B. D., Uden, P. C., Barnes, R. M., *Anal. Chem.*, 1978, 50, 2112.
10. Barret, P., Copeland, T. R., 5th FACSS Meeting; Boston, 1978.
11. Quimby, B. D., Delaney, M. F., Uden, P. C., Barnes, R. M., *Anal. Chem.*, 1979, 51, 875.
12. Rommers, P. J., Boumans, P. W. J. M., XXI CSI/8th ICAS, Cambridge, U. K., 1979.
13. Van Dalen, J. P. J., Kwee, T. G., DeGalan, L., XXI CSI/8th ICAS, Cambridge, U. K., 1979.
14. Mulligan, K. J., Hahn, M. H., Caruso, J. A., Fricke, F. L., *Anal. Chem.*, 1979, 51, 1935.
15. Zander, A. T., Hieftje, G. M., 30th Pitts. Conf. on Anal. Chem. and Appl. Spec., Cleveland, OH, 1979.
16. Zander, A. T., Hieftje, G. M., XXI CSI/8th ICAS, Cambridge, U. K., 1979.
17. Zander, A. T., Hieftje, G. M., 11th Central Reg. Mtg. ACS, Columbus, OH, 1979.
18. Brasseur, P., Maessen, F. J. M. J., DeGalan, L., *Spectrochim. Acta*, 1976, 31B, 537.
19. Serravallo, F. A., Risby, T. H., *Anal. Chem.*, 1975, 47, 2141.
20. Lampe, F. W., Risby, T. H., Serravallo, F. A., *Anal. Chem.*, 1977, 49, 560.

21. Van Dalen, J. P. J., DeLezenne Coulander, P. A., DeGalan, L., Anal. Chim. Acta, 1977,94,1.
22. Schwarz, F. P., Anal. Chem., 1978,50,1006.
23. Brassem, P., Maessen, F. J. M. J., DeGalan, L., Spectrochim. Acta, 1978,33B,753.
24. Schwarz, F. P., Anal. Chem., 1979,51,1508.
25. Hubert, J., Moisan, M., Ricard, A., Spectrochim. Acta, 1979,33B,1.
26. Layman, L. L., Hieftje, G. M., Anal. Chem., 1975,47,194.

FIGURE CAPTIONS

Figure 1: Excitation temperature profiles at different flow rates. Thermometric species: He

A. 1.95 L/m

B. 3.00 L/m

C. 4.11 L/m

Chamber region occupied by MIP at specified flow rates:

a. 1.95 L/m

b. 3.00 L/m

c. 4.11 L/m

Figure 2: Excitation temperature profiles at different flow rates. Thermometric species: Fe

A. 1.95 L/m

B. 3.00 L/m

C. 4.11 L/m

Chamber region occupied by MIP at specified flow rates:

a. 1.95 L/m

b. 3.00 L/m

c. 4.11 L/m

Figure 3: Relative intensity profiles for Fe I:

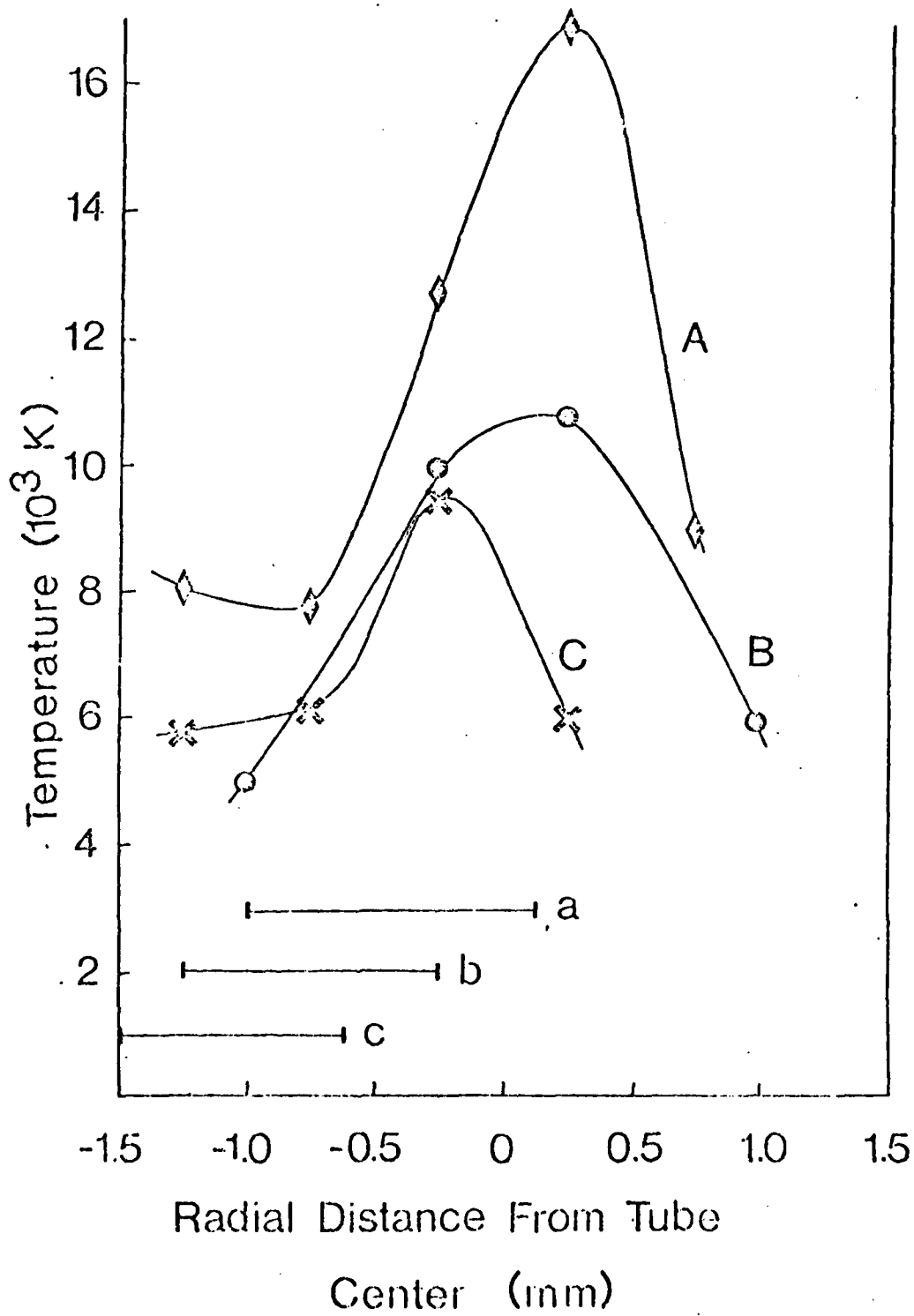
A1, B1, C1: 287.234nm

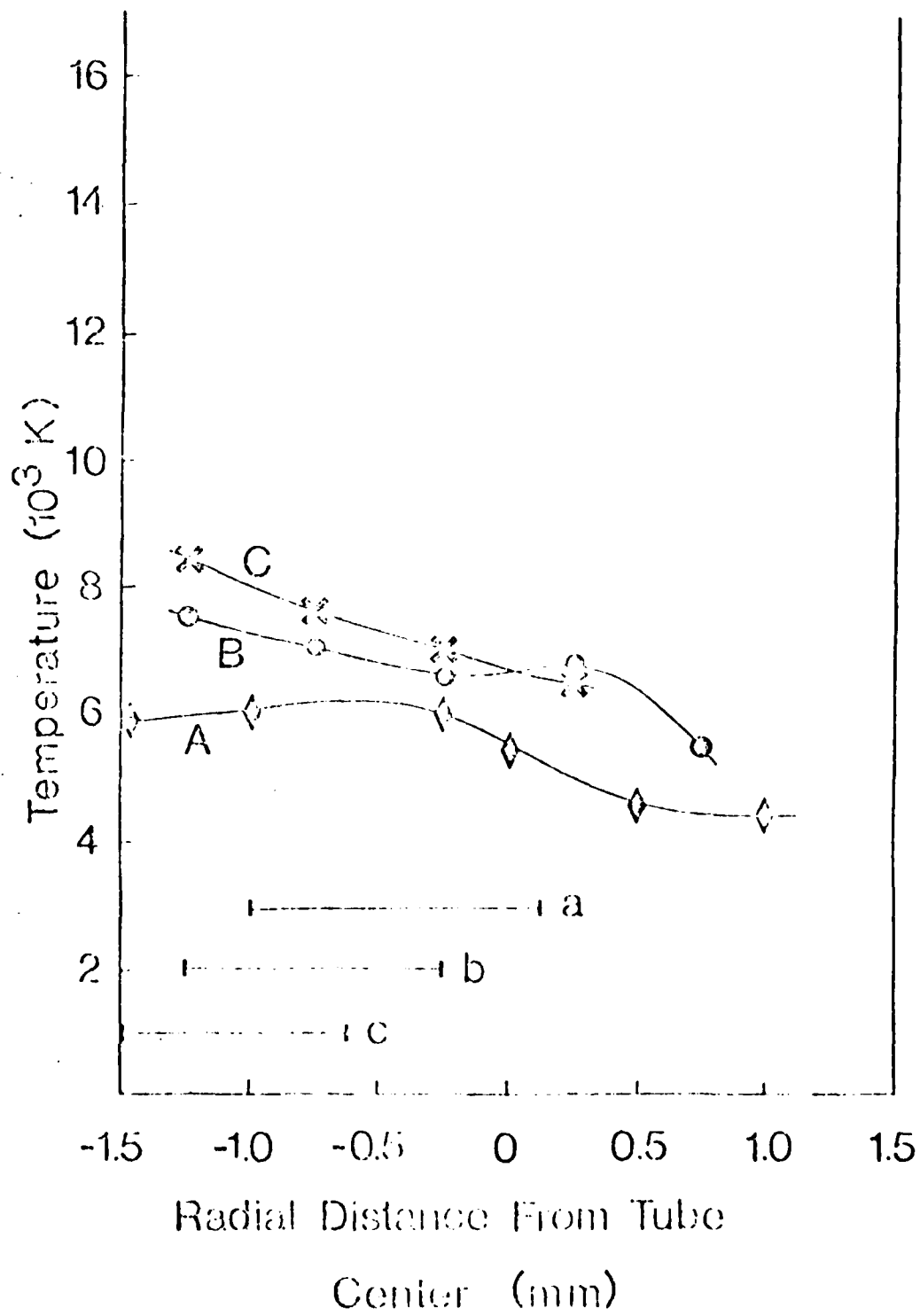
A2, B2, C2: 371.994nm

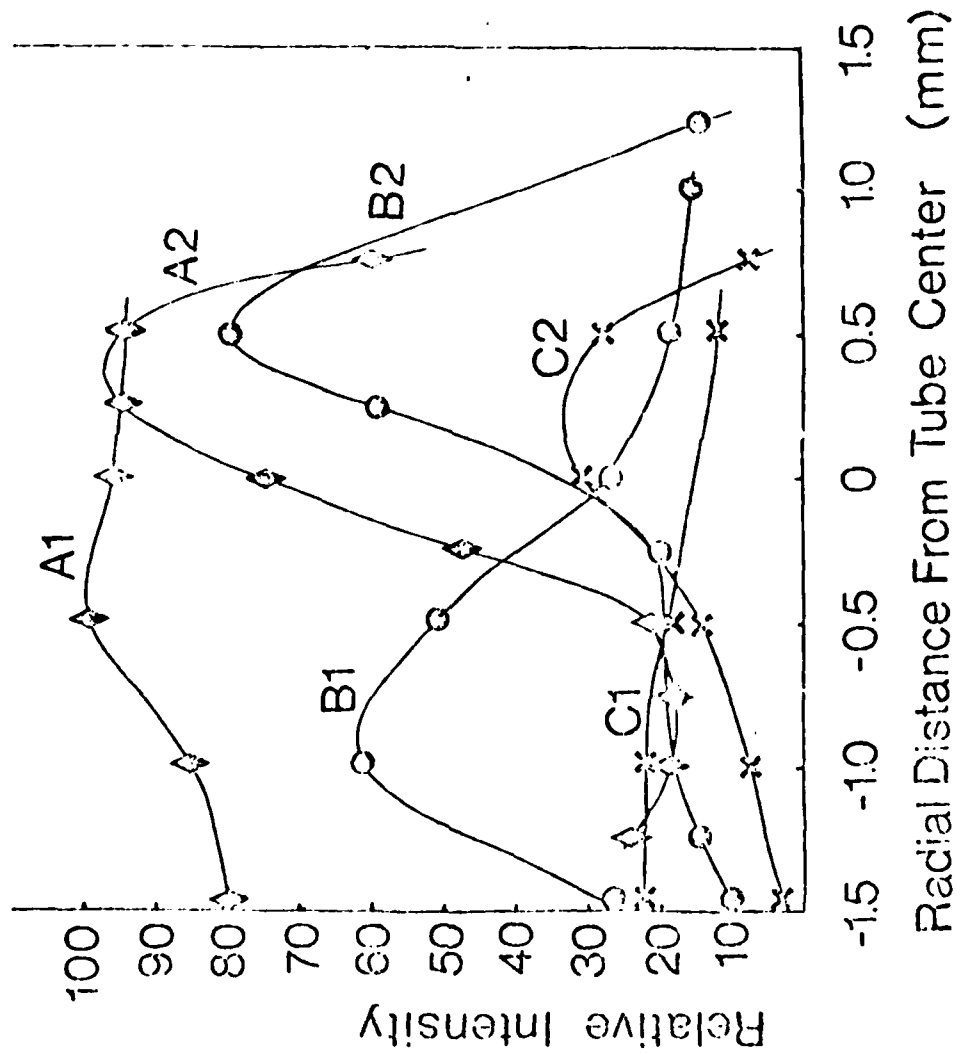
A. 1.95 L/m

B. 3.00 L/m

C. 4.11 L/m







TECHNICAL REPORT DISTRIBUTION LIST, 051C

| | <u>No.</u> <u>Copies</u> | | <u>No.</u> <u>Copies</u> |
|--|-----------------------------|--|-----------------------------|
| Dr. M. B. Denton Department of Chemistry University of Arizona Tucson, Arizona 85721 | 1 | Dr. John Duffin United States Naval Postgraduate School Monterey, California 93940 | 1 |
| Dr. R. A. Osteryoung Department of Chemistry State University of New York at Buffalo Buffalo, New York 14214 | 1 | Dr. G. M. Hieftje Department of Chemistry Indiana University Bloomington, Indiana 47401 | 1 |
| Dr. B. K. Kowalski Department of Chemistry University of Washington Seattle, Washington 98105 | 1 | Dr. Victor L. Rehn Naval Weapons Center Code 3813 China Lake, California 93555 | 1 |
| Dr. S. P. Perone Department of Chemistry Purdue University Lafayette, Indiana 47907 | 1 | Dr. Christie G. Enke Michigan State University Department of Chemistry East Lansing, Michigan 48824 | 1 |
| Dr. D. L. Venezky Naval Research Laboratory Code 6130 Washington, D.C. 20375 | 1 | Dr. Kent Eisentraut, MBT Air Force Materials Laboratory Wright-Patterson AFB, Ohio 45433 | 1 |
| Dr. H. Freiser Department of Chemistry University of Arizona Tucson, Arizona 85721 | | Walter G. Cox, Code 3632 Naval Underwater Systems Center Building 148 Newport, Rhode Island 02840 | 1 |
| Dr. Fred Saalfeld Naval Research Laboratory Code 6110 Washington, D.C. 20375 | 1 | Professor Isiah M. Warner Texas A&M University Department of Chemistry College Station, Texas 77840 | 1 |
| Dr. H. Chernoff Department of Mathematics Massachusetts Institute of Technology Cambridge, Massachusetts 02139 | 1 | Professor George H. Morrison Cornell University Department of Chemistry Ithaca, New York 14853 | 1 |
| Dr. K. Wilson Department of Chemistry University of California, San Diego La Jolla, California | 1 | Dr. Rudolph J. Marcus Office of Naval Research Scientific Liaison Group American Embassy APO San Francisco 96503 | 1 |
| Dr. A. Zirino Naval Undersea Center San Diego, California 92132 | 1 | Mr. James Kelley DTNSRDC Code 2803 Annapolis, Maryland 21402 | 1 |

TECHNICAL REPORT DISTRIBUTION LIST, GEN

| | <u>No.</u> <u>Copies</u> | | <u>No.</u> <u>Copies</u> |
|---|-----------------------------|---|-----------------------------|
| Office of Naval Research Attn: Code 472 800 North Quincy Street Arlington, Virginia 22217 | 2 | U.S. Army Research Office Attn: CRD-AA-IP P.O. Box 1211 Research Triangle Park, N.C. 27709 | 1 |
| ONR Branch Office Attn: Dr. George Sandoz 536 S. Clark Street Chicago, Illinois 60605 | 1 | Naval Ocean Systems Center Attn: Mr. Joe McCartney San Diego, California 92152 | 1 |
| ONR Area Office Attn: Scientific Dept. 715 Broadway New York, New York 10003 | 1 | Naval Weapons Center Attn: Dr. A. B. Amster, Chemistry Division China Lake, California 93555 | 1 |
| ONR Western Regional Office 1030 East Green Street Pasadena, California 91106 | 1 | Naval Civil Engineering Laboratory Attn: Dr. R. W. Drisko Port Hueneme, California 93401 | 1 |
| ONR Eastern/Central Regional Office Attn: Dr. L. H. Peebles Building 114, Section D 666 Summer Street Boston, Massachusetts 02210 | 1 | Department of Physics & Chemistry Naval Postgraduate School Monterey, California 93940 | 1 |
| Director, Naval Research Laboratory Attn: Code 6100 Washington, D.C. 20390 | 1 | Dr. A. L. Slafkosky Scientific Advisor Commandant of the Marine Corps (Code RD-1) Washington, D.C. 20380 | 1 |
| The Assistant Secretary of the Navy (RE&S) Department of the Navy Room 4E736, Pentagon Washington, D.C. 20350 | 1 | Office of Naval Research Attn: Dr. Richard S. Miller 800 N. Quincy Street Arlington, Virginia 22217 | 1 |
| Commander, Naval Air Systems Command Attn: Code 3100 (H. Rosenwasser) Department of the Navy Washington, D.C. 20360 | 1 | Naval Ship Research and Development Center Attn: Dr. G. Bosmajian, Applied Chemistry Division Annapolis, Maryland 21401 | 1 |
| Defense Technical Information Center Building 5, Cameron Station Alexandria, Virginia 22314 | 12 | Naval Ocean Systems Center Attn: Dr. S. Yamamoto, Marine Sciences Division San Diego, California 91232 | 1 |
| Dr. Fred Saffield Chemistry Division, Code 6100 Naval Research Laboratory Washington, D.C. 20375 | 1 | Mr. John Boyle Materials Branch Naval Ship Engineering Center Philadelphia, Pennsylvania 19112 | 1 |